

We are IntechOpen, the world's leading publisher of Open Access books Built by scientists, for scientists

4,800

Open access books available

122,000

International authors and editors

135M

Downloads

Our authors are among the

154

Countries delivered to

TOP 1%

most cited scientists

12.2%

Contributors from top 500 universities



WEB OF SCIENCE™

Selection of our books indexed in the Book Citation Index
in Web of Science™ Core Collection (BKCI)

Interested in publishing with us?
Contact book.department@intechopen.com

Numbers displayed above are based on latest data collected.

For more information visit www.intechopen.com



Modeling of Hydrogen Absorption/Desorption in a Metal Hydride Bed Reactor — A Theoretical Study

Olaitan Akanji and Andrei Kolesnikov

Additional information is available at the end of the chapter

<http://dx.doi.org/10.5772/61625>

Abstract

Hydrogen has been considered as an alternative source of fuel to the fossil fuel in future, most especially, for mobile applications. However, a requirement is the safe, efficient and compact on-board storage of hydrogen. Reversible storage in metal hydride is promising, but adequate knowledge of materials system fulfills all requirements regarding hydrogen content is a major drawback, release temperature, and reversibility simultaneously. Hydrogen absorption-desorption in a metal hydride bed reactor can be modeled using different software such as FLUENT, CFD-ACE, and COMSOL Multiphysics. This book chapter will focus on the use of software COMSOL Multiphysics to simulate the diffusion and heating of hydrogen and metal hydride powder in both radial and axial directions. The model consists of system of partial differential equations (PDE) describing two-dimensional heat and mass transfer of hydrogen in a porous matrix. The influence of the operating parameters Temperature, Pressure, Concentration, Permeability and Thermal Conductivity on the rate of absorption-desorption of hydrogen in metal hydride will be fully discussed. The simulation results obtained could be applied to the on-board hydrogen storage technology, in particular for the hydrogen supply of a fuel cell for powering of a hydrogen fuel cell vehicle.

Keywords: Hydrogen, Storage, Metal hydride, Absorption, Desorption

1. Introduction

The excessive demand of Energy across the globe has risen sharply over the last decade. Today, fossil-fuel-based sources of energy are being depleted at a fast rate because of the ever

increasing energy demand and consumption. In addition, fossil-fuels are contributing to both greenhouse gas emissions and global warming [1]. Due to these hazardous effects, there should be an urgent need for alternative and cleaner fuels which will be toxin free and environmentally friendly. Hydrogen energy seems to be the best alternative for the future to replace the fossil fuel and it already has several applications such as in heat pumps and automotive industries. One of the main problems in large usage of hydrogen in automotive industry is the storage problem. The conventional hydrogen storage methods in use for hydrogen gases are gas compression and liquefaction. These storage methods are impractical since the former requires very heavy gas tank and the latter is too expensive to be implemented in public vehicles. Storing hydrogen in metal hydride beds as a chemical compound appears to be a method of hydrogen storage in near future, and as this has received much interest recently [2]. There are several important challenges to overcome before hydrogen can become a viable fuel. Only 1% of the hydrogen is available as molecular hydrogen gas while the majority is present in the form of water or hydrocarbons. The large-scale production of hydrogen from water or chemical compounds in an efficient and clean method remains a challenge. Another challenge is storage volume. Although hydrogen has high energy content by weight (three times that of gasoline), its energy content by volume is only one-tenth that of gasoline. The process is a major storage volume problem in automotive and other mobile systems with stringent volume constraint. A third challenge is hydrogen transport to filling stations. Because of the low density of hydrogen, finding an economical way of transporting large amounts of hydrogen to various locations is quite illusive. The fourth challenge is the use of hydrogen as a fuel in producing clean energy that would justify its wide acceptance in the market [1]. Hydrogen can be used to produce energy either by burning with oxygen in air (e.g. internal combustion engine) or by electrochemical reaction with oxygen using fuel cells. Fuel cells are both energy efficient and virtually pollution free compared to internal combustion engines. The choice of energy production method is dictated mainly by cost and application. A promising alternative method of storing hydrogen in a fuel cell is solid-metal hydride storage utilizing metal hydride to absorb/desorb hydrogen at a relatively low pressure (<20-bar), which offers safety and cost advantage, but the obvious disadvantage of weight for hydrogen onboard storage. Efficient release of hydrogen gas in the metal hydride reactor should meet the need for fast load variation in order to build and satisfy such hydrogen systems. The physics of the transport process coupled with reaction kinetics are very important such as hydrogen mass flow in the hydride bed, heat transfer within the bed and local hydrogen absorption rate. - [3]. Several mathematical models for analyzing hydrogen absorption/desorption in metal hydride beds were presented in the literature:

Jemni and Nasrallah [3] presented a model for the two-dimensional transient heat and mass transfer within a cylindrical reactor. The influence of some parameters (reactor radius, temperature and inlet pressure) on the dynamic reactor performance was determined.

Aldas et al. [4] extended the mathematical model of Jemni and Nasrallah to three-dimensions demonstrating that hydrogen flow significantly influences the temperature profile in the system

Mayer et al. [5] - developed a one-dimensional model which showed that heat and mass transfer are key factors affecting reaction rate in the reactor.

Nakawaga et al.[6]- predicted the transient heat and mass transfer phenomenon through the hydride bed by using a two-dimensional mathematical model with hydriding and dehydriding kinetics.

2. Methodology

Those equations, which represent the mathematical model of hydrogen absorption/desorption in metal hydride, are stated here, and implemented in COMSOL MULTIPHYSICS software to validate the experiment performed by Jemni et al. [9] and the following parameters were determined:

- Temperature variation during charging and discharging of hydrogen in metal hydride reactor
- Variation in the density of metal hydride in the reactor during hydrogen charging and discharging
- Variation in the pressure of hydrogen in metal hydride reactor during charging and discharging
- Variation in the flow rate of the gas at the outlet of the metal hydride reactor

2.1. Mass balance

The mass conservation equation of the solid metal hydride is presented as follows:

$$(1 - \varepsilon) \frac{\partial \rho_s}{\partial t} = m \quad (1)$$

In Equation (1), the left side represents the accumulation/dissipation term for mass of metal hydride, and the term on the right side represents mass of metal hydride release during adsorption/desorption.

Mass balance equation for hydrogen gas is given by equation (2):-

$$\varepsilon \frac{\partial \rho_g}{\partial t} + \nabla(\rho_g u_g) = m \quad (2)$$

In Equation (2), the term $\varepsilon \frac{\partial \rho_g}{\partial t}$ - represents accumulation/dissipation term for hydrogen gas release during adsorption/desorption and the second term on the left side represents convection transfer. The term on the right side represents amount of hydrogen gas release during absorption/desorption.

$$u_g = \frac{K}{\mu_g} \nabla P_g \quad (3)$$

Equation (3) is called Darcy equation, and the velocity of hydrogen gas is calculated from this equation. The equation term on the left side represents the velocity of the gas and the right-hand side of the equation represents Darcy expression.

$$m = C_d \exp\left(-\frac{E_d}{R_g T}\right) \frac{P_g - P_{eq}}{P_{eq}} \rho_s \quad (4)$$

The hydrogen release/consumption due to absorption/desorption is given by Equation (4). The term on the left side represents the amount of hydrogen gas released during absorption/desorption and the equation term on the right side represents the kinetic of absorption/desorption of hydrogen.

2.2. Momentum balance and equilibrium pressure

Jemni et al. [3],- proposed the following equilibrium pressure equation

$$\ln(P_{eq}) = \frac{\Delta H}{RT} - \frac{\Delta S}{R} + (\varphi - \phi_0) \tan\left[\pi\left(\frac{C}{C_m} - \frac{1}{2}\right)\right] + \frac{\beta}{2} \quad (5)$$

In Equation (5), the term on the left side represents equilibrium pressure. Vant Hoff derived the right-hand side expression, the second term to the right is known as plateau value, and the last term to the right is called hysteresis value.

$$\frac{\partial(\rho_g \varepsilon)}{\partial t} + \nabla \cdot \left(-\rho_g \frac{K}{\mu_g} \nabla P_g\right) = 0 \quad (6)$$

Equation (6), - represents the momentum balance, the first term to the left represents change in momentum due to non-stationary equilibrium and the second term to the left represents momentum change due to absorption inside the porous medium.

$$K = C_k \cdot d_p^2 \left(\frac{\varepsilon}{1 - \varepsilon}\right)^2$$

Permeability K and porosity are related Equation (6) above, where d_p is metal hydride particle diameter and constant $Ck=2.37 \times 10^{-3}$.

2.3. Energy balance

Energy balance is written in assumption that porous metal hydride bed and hydrogen gas are having the same temperature.

Energy balance equation (7) describes temperature evolution of the hydrogen porous bed system-:

$$\frac{d}{dt} \left(\varepsilon \rho_g C_{pg} T + (1 - \varepsilon) \rho_s C_{ps} T - \varepsilon \frac{\rho_g RT}{M_{H_2}} \right) + \nabla \cdot (\rho_g C_{pg} u T - \lambda_e \nabla T) + (1 - \varepsilon) (-\Delta H) \rho_s m = 0 \quad (7)$$

The first term in Equation (7) to the left represents unsteady heat change in the system, and second term to the left represents heat change in the system due to conduction and third term to the left represents heat release/consumption due to chemical reaction in absorption-desorption processes.

Effective thermal conductivity of metal hydride bed is expressed as:

$$\lambda_e = \varepsilon \lambda_g + (1 - \varepsilon) \lambda_s \quad (8)$$

2.4. Conclusion

The dynamic model of the process incorporates coupling between hydrogen adsorption/desorption, flow in porous media, and heat transfer in porous media and gas. The model also assumes thermal equilibrium between metal hydride (solid phase) and hydrogen (gas phase). The equations are implemented in computational software COMSOL 4.0a to solve for dependent variables such as temperature, metal hydride density, gas pressure, and velocity of the gas.

2.5. Building the geometry

The geometry for the MHHST was presented as a cylindrical reactor where hydrogen is adsorbed/desorbed in/out of metal-hydride powder stored in the reactor. Because of axial symmetry, 2D model was used.

In COMSOL software, the geometry was built in the form of rectangles, and final geometry was developed by the Boolean operations: forming union of three different rectangles and then finding the Boolean differences.

One rectangle represents domain for hydrogen, the second rectangle represents the domain for metal-hydride that will absorb/desorb hydrogen, and the third rectangle represents the domain that will supply heat to the system. The material used in for the tank walls is copper due to its high conductivity. Copper walls were built as an envelope surrounding the metal hydride rectangles. The contour line of the tank was built from certain geometrical points. The points have different coordinates listed in the Table 1. The geometry of the tank is shown in Figure 1. It can be seen that the tank has two radial ribs/fins for better thermal management.

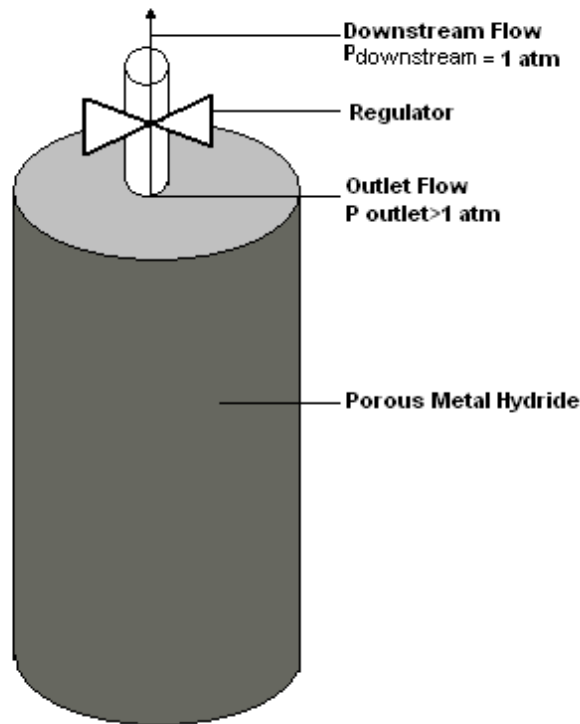


Figure 1. Schematic of Metal hydride reactor.

| R- coordinates | Z- coordinates |
|----------------|----------------|
| 0.025 | 0 |
| 0.025 | 0.05 |
| 0.025 | 0.075 |
| 0.025 | 0.15 |
| 0.025 | 0.175 |
| 0.025 | 0.24 |
| 0.05 | 0.05 |
| 0.05 | 0.075 |

| R- coordinates | Z- coordinates |
|----------------|----------------|
| 0.05 | 0.15 |
| 0.05 | 0.175 |

Table 1. Geometry Coordinates

2.6. Computational mesh

Figure 2 shows the mesh of the MHHST and different boundaries. The portion of the MHHST is taken as rectangular shape that comprises two computational domains (1 and 2). Domain 1 represents metal hydride insulated with copper body (Domain 2), which serves as a conductor to supply/remove heat from metal hydride bed. The heat is supplied to metal hydride (or removed) through the copper walls.

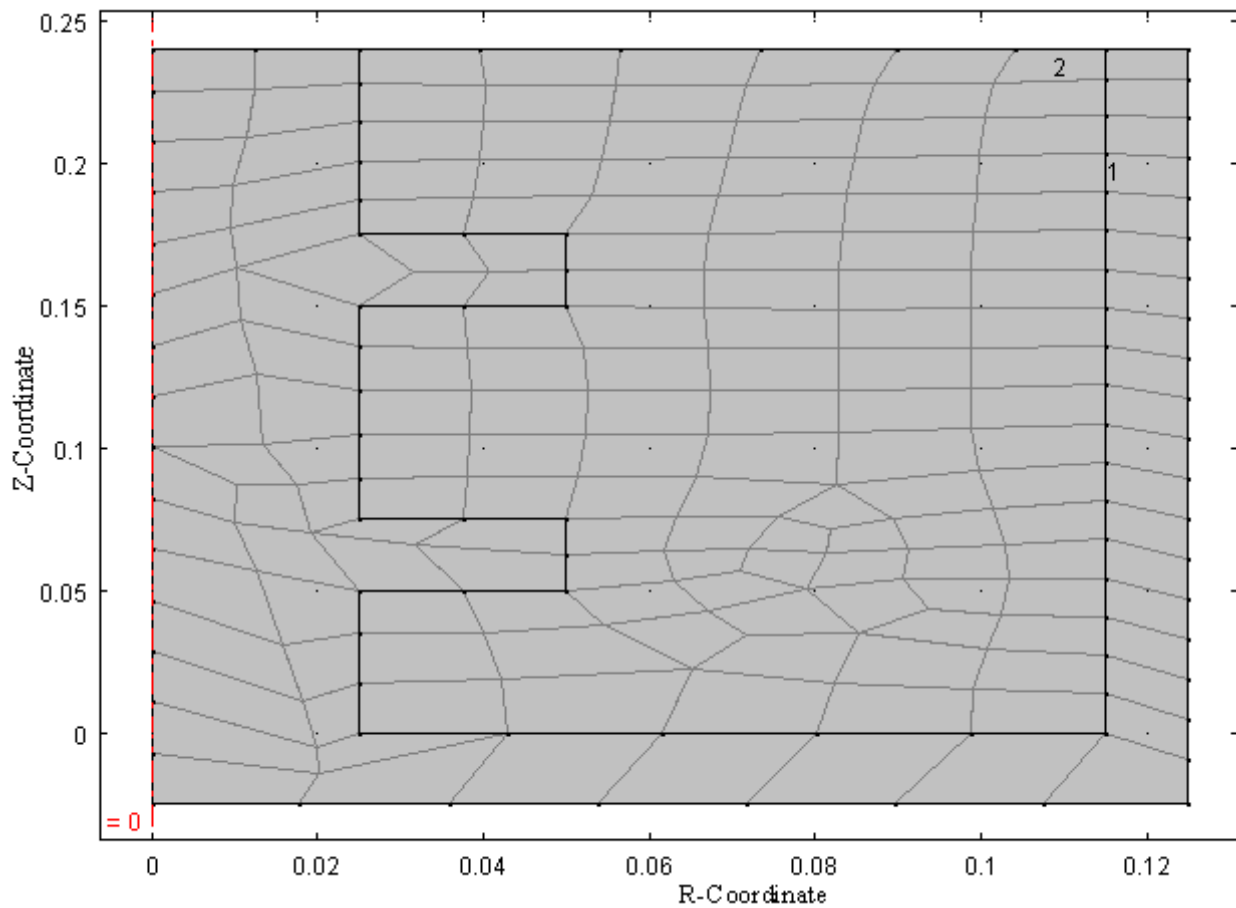


Figure 2. Computational Mesh.

2.7. Boundary conditions

The boundary conditions are described in Figure 3.

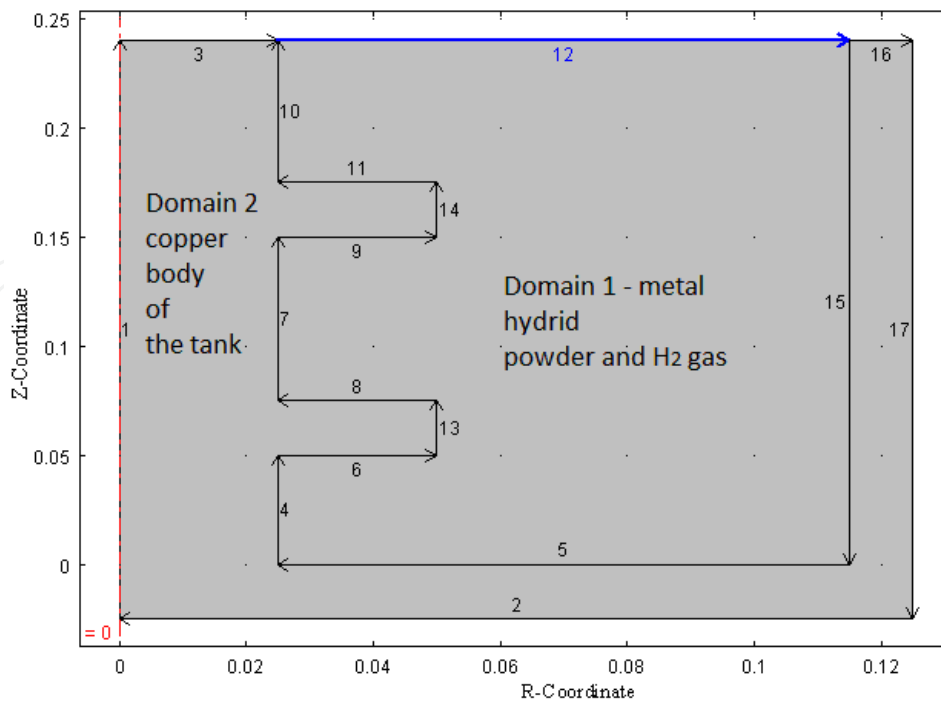


Figure 3. Boundaries within MHHST during hydrogen absorption and desorption

Figure 3. shows different boundaries within MHHST. Each boundary illustrates the heat and mass transfer of hydrogen during absorption and desorption.

The Following types of boundary conditions were used.

For modeling of heat transfer during absorption:

- a. inlet/outlet –Boundary 12
- b. wall – Boundary 9, 14...
- c. flux – Boundary 9...
- d. isolation – Boundary 9...

For modeling of momentum transfer during absorption:

- a. inlet/outlet
- b. wall
- c. flux
- d. isolation

For modeling of hydrogen diffusion during absorption:

- a. inlet/outlet Pressure $P = 40_bar_ (absorption)$ or $10_bar_ (desorption)$
- b. wall - $C=C_{wall} = 293_K$

- c. flux $Q = \dots h \cdot (T_{\text{ext}} - T)$ mol/m²
- d. isolation - $dC/dz = 0$

For modeling of heat transfer during desorption:

- a. inlet- outlet – Boundary 12
- b. wall–Boundary 9, Boundary 14, Boundary 16, $T = 293_K$
- c. flux – boundary 9 $Q = \dots h \cdot (T_{\text{ext}} - T)$ W/m²
- d. Isolation – Boundary 9, Boundary 10, Boundary 11–. $dT/dz = 0$

For modeling of momentum transfer during desorption:

- a. inlet/outlet
- b. Wall
- c. Flux
- d. Isolation

For modeling of hydrogen released during desorption:

- a. inlet/outlet Pressure $P = 8_bar$
- b. wall, $C = C_{\text{wall}} = \rho_{\text{sat}}/Mg$ (mol/m³)
- c. flux $Q = h \cdot (T_{\text{ext}} - T)$ (mol/m³)/m²
- d. isolation, $dC/dz = 0$

2.8. Initial conditions

At the beginning of the absorption, the system is at 293_K and the hydrogen is injected at the top of the system (Boundary 12) with the pressure $P = 40_bar$, then the hydride absorbs and the exothermic reaction raises the temperature.

At the beginning of the desorption, the system is at 333_K and the hydrogen is released from the MHHST through the outlet of the system (Boundary 12) with the pressure $P = 10_bar$. The temperature decreases slowly within the tank, due to the endothermic reaction, then hydrogen desorbs slowly from the hydride.

2.9. Simulation variables, parameters, and function used

The mathematical model is applied to the geometry built above and various variables parameter and functions used from the experimental work performed by Jemni et al (1995) are defined specifically and solved with the aid of COMSOL MULTIPHYSICS software. The density of metal hydride presented in the table for this research work is bulk densities (Table 2)

| | | |
|---------|-----------------------------|---|
| rho_s | 6360_[kg/m ³] | Bulk density of metal hydride at saturation |
| rho_emp | - 6000[kg/m ³] | Bulk density of metal hydride |
| Cps | - 419[j/kg/k] | Solid- specific heat capacity |
| Cpg | - 14890[j/kg/k] | Gas- specific heat capacity |
| k_e | - 1.32[w/m/k] | effective thermal conductivity |
| K | - 1e_08 | permeability |
| epsilon | 0.5 | porosity |
| Mg | 2.01588_03_[kg/mol] | hydrogen molecular weight |
| Rg | - 8.314[J/mol/k] | universal gas constant |
| ca | - 59.187_[1/s] | absorption constant |
| cd | - 9.57_[1/s] | desorption constant |
| Ea | - 21179.6[J/mol] | absorption activation energy |
| Ed | - 15473_[J/mol] | desorption activation energy |
| T_ini | - 293_[k] | initial temperature |
| P_ini | 156000_[Pa] | initial pressure |
| deltaH | -1.539e+07_[J/kg] | heat of formation in abs/des reaction |
| eta | - 9.2e-06_[Pa*S] | dynamic viscosity |
| h1 | - 150_[w/m ² /k] | heat source |
| v_out | - 1.098_[m/s] | outlet velocity |
| Po | - 18_[bar] | initial Pressure |
| P | - 50_[bar] | Pressure |
| Pg | - P_[Pa] | gas pressure from Darcy |
| Cps | - 419_[j/kg/K] | Solid specific heat capacity |

Table 2. Variables and function used in simulation (Jemni et al. [3])

The developed mathematical model included the following variables and functions, which were used to simulate heat and mass transfer inside hydrogen storage tank. The variables and functions are listed in the Table 3 below.

| | | |
|---------|---------------------------|-----------------------------|
| T_ini | 293_[K] | Initial temperature |
| p_ini | 143,220_[Pa] | Initial pressure |
| c_ini | rho_emp/Mg | Initial concentration |
| rho_s | c.*Mg | Current density of solid MH |
| rho_sat | 8527_[kg/m ³] | Saturated density |

| | | |
|-----------|---|---------------------------------------|
| rho_emp | 8400_[kg/m ³] | Empty density |
| Cps | 419_[J/kg/K] | Solid specific heat |
| Cpg | 14890_[J/kg/K] | Gas specific heat |
| k_e | 1.32_[W/m/K] | Effective thermal conductivity |
| K | 1e-08_[m ²] | Permeability |
| deltaH | -1.539e+07_[J/kg] | Heat of formation in abs/des reaction |
| epsilon | 0.5 | Porosity of the gas |
| Mg | 2.01588e-03[kg/mol] | H2 mol weight |
| Rg | 8.314[J/mol/K] | Universal gas constant |
| Ca | 59.187[1/s] | Absorption constant |
| Cd | 9.57[1/s] | Desorption constant |
| Ea | 21179.6[J/mol] | Absorption activation energy |
| Ed | 15473_[J/mol] | Desorption activation energy |
| Pg | p | Gas pressure |
| Peqa | 1000[Pa]*exp(17.6083704.6[K]/T) | Equilibrium pressure of absorption |
| Peqd | 1000[Pa]*exp(17.4783704.6[K]/T) | Equilibrium pressure of desorption |
| m_des_fin | if(Pg<Peqd,Cd*exp(Ed/(Rg*T)) *(g-Peqd)/Peqd*(rho_s-rho_emp),0) | Mass source during desorption process |
| m_abs_fin | if(Pg"/>=Peqa,(Ca*exp(Ea/(Rg*T)) *log(Pg/Peqa)*(rho_sat-rho_s)),0) | Mass source during absorption process |
| m1 | if(abs(m_des_fin)"/> >abs(m_abs_fin),m_des_fin,m_abs_fin) | Auxiliary term |
| M | if(((m_des_fin==0)&&(m_abs_fin==0)), 0,m1) | Total mass source/sink |

Table 3. Simulation variables and functions

2.10. Model verification

To validate the model, the results of Jemni et al.[3] were used. The simulation results obtained were compared with one obtained by Jemni et al. [10]. The comparison of the axial temperature distribution in the paper of Jemni and the calculated results shows agreement with each other. (Figure 4).

Further modification of simulation variables and functions used by Jemni et al. with introduction of some conditions upon simulation produced similar results, which can be shown in the Figures 5 and 6. The main body of results obtained in current research is given in the following Chapter.

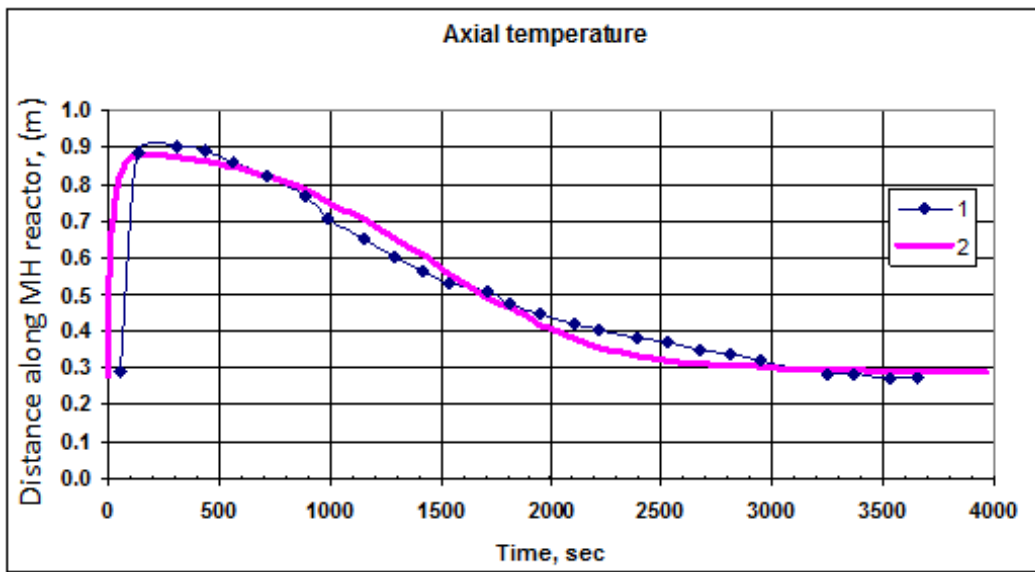


Figure 4. Axial temperature distribution in metal hydride reactor. 1 – Experiment (Jemni et. al. [3]-), 2 – calculations.

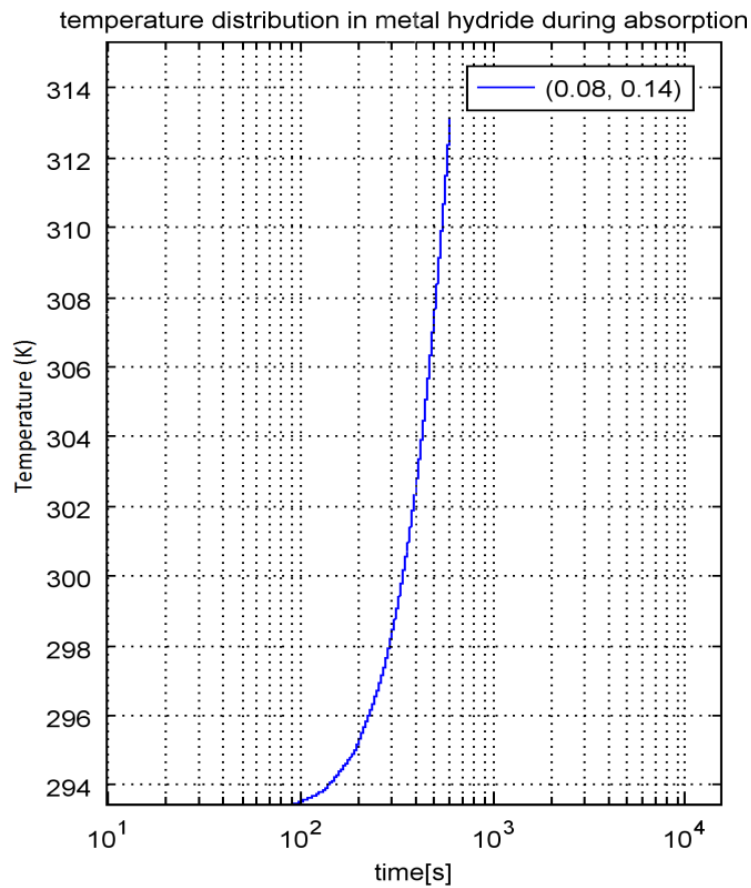


Figure 5. Time evolution of temperature in metal hydride reactor during absorption at point with coordinates [0.08, 0.14] during the 600-s period.

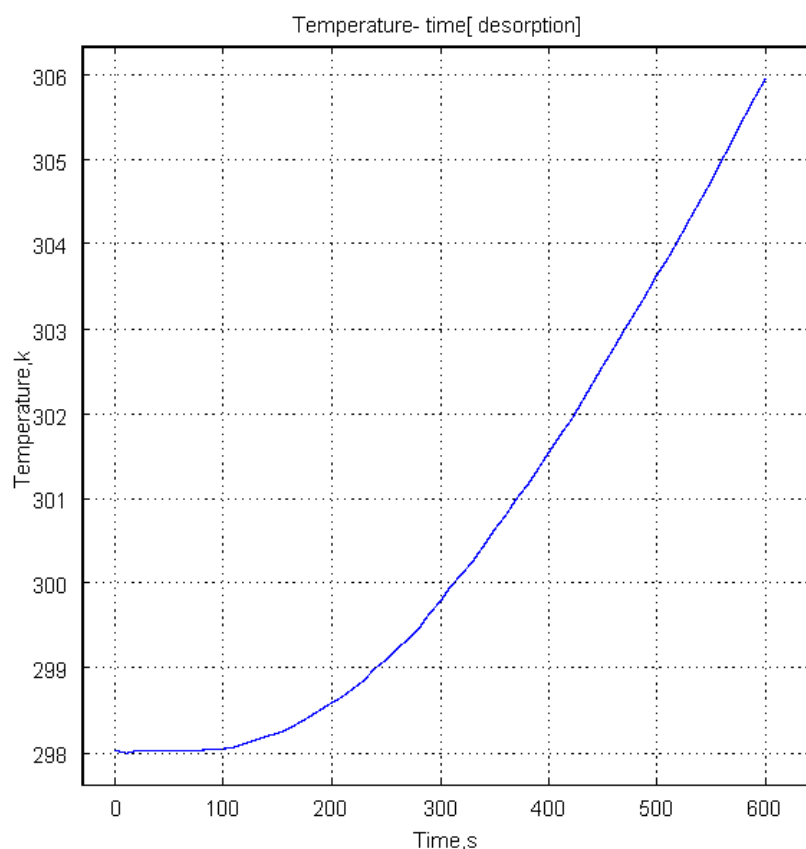


Figure 6. Time evolution of temperature in metal hydride reactor during desorption at point with coordinates [0.08, 0.14] during the 600-s period.

There is a significant - agreement between the results obtained by Jemni et al. [3], and the simulation for this work, for both absorption and desorption process. While Jemni et al. [10] used the cylindrical tank as a reactor for metal hydride hydrogen storage, in this work, most of the simulations were performed for the reactor with - rectangular fins.

3. Results and discussion

3.1. Dynamics of absorption process

Absorption process was simulated for hydrogen storage tank filled with AB_5 type metal hydride. The geometry of the tank and the boundary conditions were described in the sections 3.1 and 3.3. The position of the sensor (measurement point) for temperature, pressure, velocity, and density has the following coordinates: radial coordinate $r=0.08$ m, axial coordinate $z=0.14$ m, which is approximately in the center of the metal hydride bed(Domain 1).

3.1.1. Temperature time distribution

Figure 7. illustrates the temperature distribution of hydrogen in MHHST during absorption at point [0.08, 0.14] of the bed. The simulation results show a gradual increase in temperature

at different time interval. The total simulation time was taken to be 600_s. The temperature at initial stage of the reaction was very slow but started to increase gradually from 200_s to 600_s, due to the exothermic nature of the reaction between hydrogen and metal hydride. More heat has been release into the bed and this tends to increase the temperature of the heating fluid. A maximum temperature of 313K within the bed was reached.

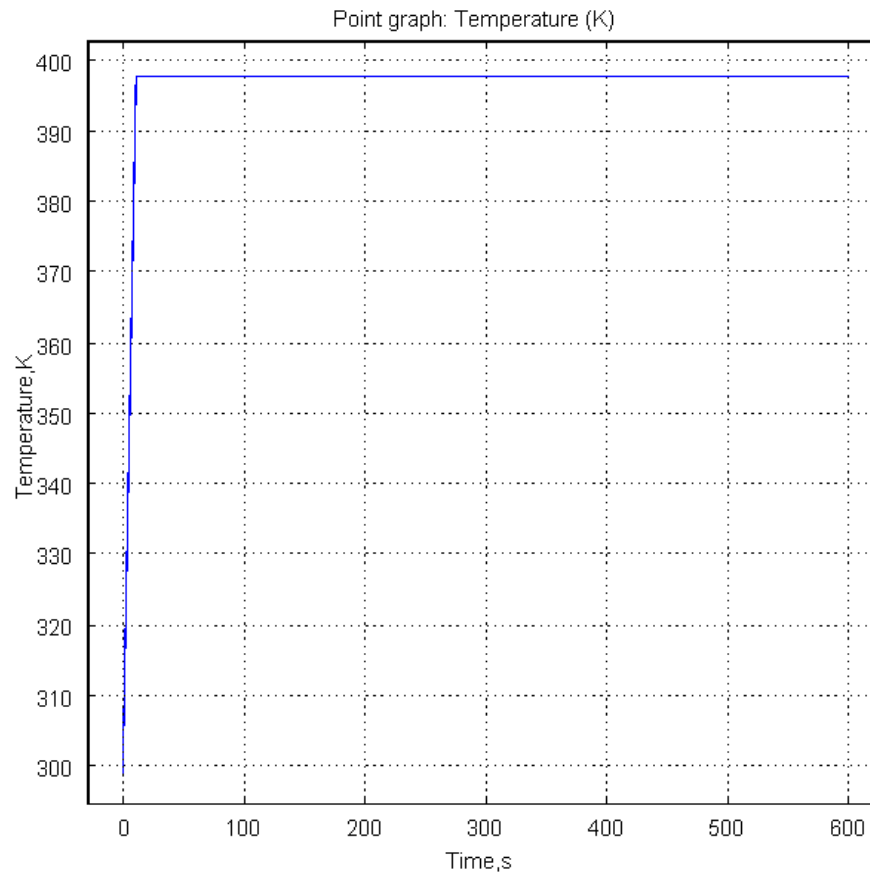


Figure 7. Time evolution of temperature in metal hydride reactor at point with coordinates [0.08, 0.14] during the 600-s period.

3.1.2. Pressure distribution

Figure 8. shows the pressure variation with time at point [0.08, 0.14] within the MHHST during absorption reaction of hydrogen. It was observed that there is an increase in the pressure in the bed during absorption process at various simulation times. More hydrogen was absorbed due to increase in temperature and pressure in the MHHST bed, which was due to the exothermic nature of the reaction. The pressure increased gradually from initial stage of the reaction, which was 0_s to final time of 600_s. At this time, the maximum pressure was reached in the bed, which is closer to the equilibrium pressure. The equilibrium pressure is $1000_{[Pa]} \cdot \exp[17.6083704.6[K]/T]$, in which the temperature T is 273_K, the temperature in the middle of the reactor. Lower temperature yields more hydrogen, and the heat released during

reaction slows down subsequent reaction for higher coolant temperature. In addition, the higher the charging pressure, the faster the reaction rate.

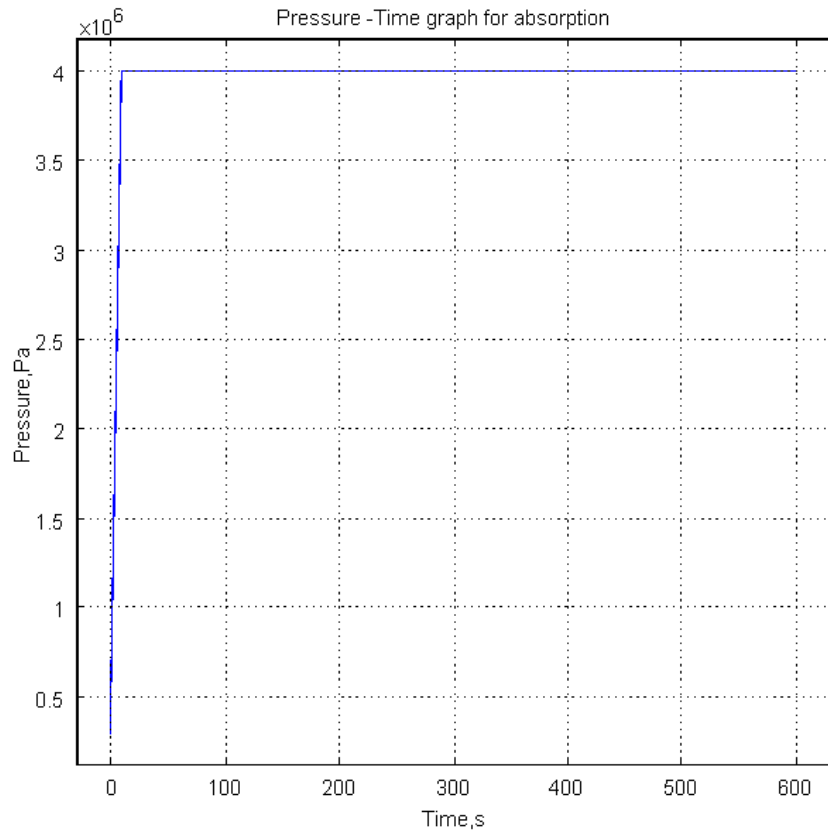


Figure 8. Time evolution of pressure in metal hydride bed at point with coordinates [0.08, 0.14] during the 600-s

3.1.3. Concentration distribution

Figure 9. illustrates the changes in the concentration of metal hydride when it absorbs hydrogen at different time intervals. It was observed that the mass of metal hydride that was loaded inside the bed changes with time gradually. At initial stage of the reaction, the concentration of metal hydride is 4.2, this value reduces to 4.225×10^6 at the final simulation time of 600_s. It can be concluded that at increasing time of the simulation, the concentration of metal hydride in the bed will decrease further when fully absorbed hydrogen.

3.1.4. Hydrogen flow rate during absorption

Figure 10. illustrates the flow rate of hydrogen into MHHST at different time interval during absorption. The flow of hydrogen into the metal hydride tends to increase with time. At the point [0.08, 0.14] of the bed, the flow rate started to increase from 0 to 0.0025kg/s and further increased to the maximum flow at a simulation time of 600s, where there is a larger absorption of hydrogen in MHHST. It can be concluded that flow rate of hydrogen into MHHST tends to increase with an increasing simulation time and a larger heat transfer coefficient values.

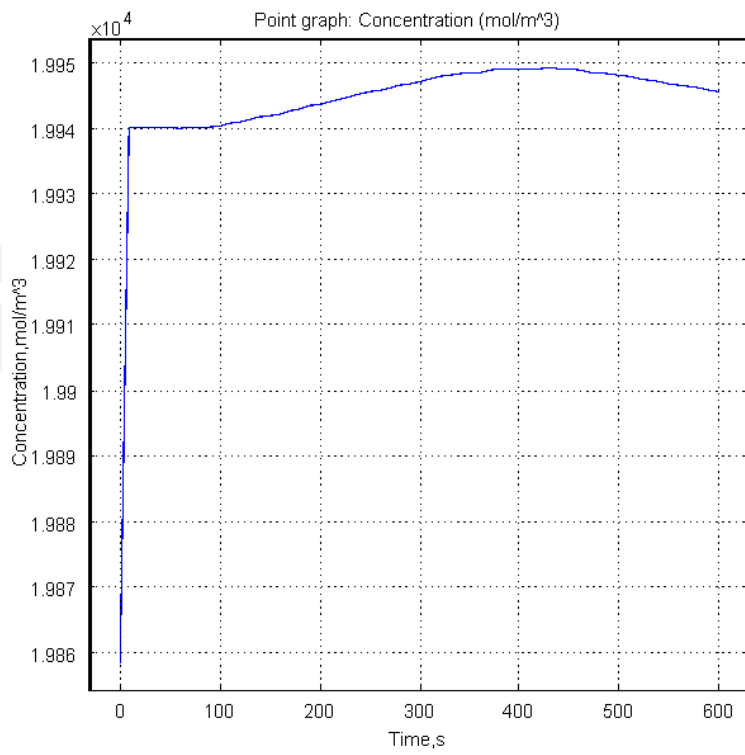


Figure 9. Time evolution of metal hydride concentration at the point with coordinates [0.08, 0.14] during the 600-s period

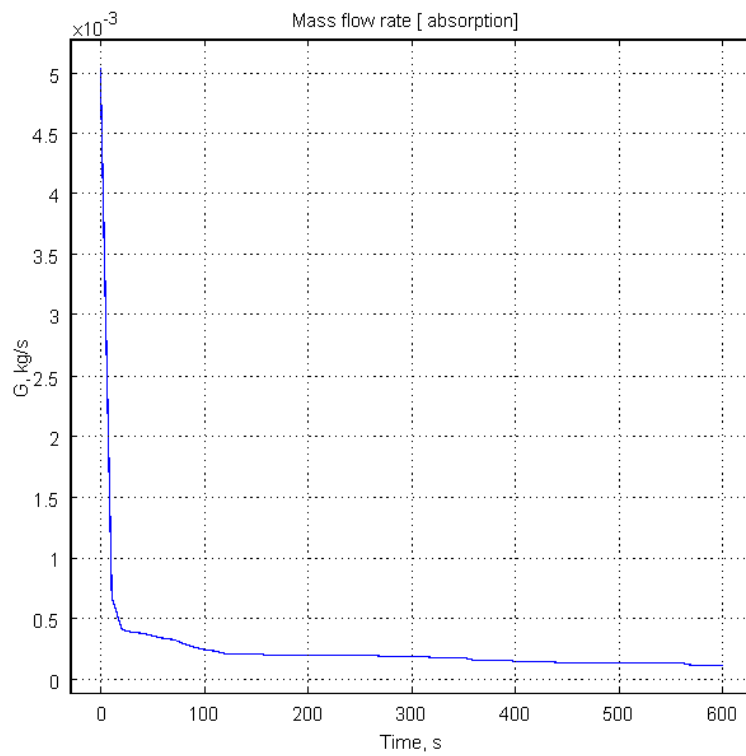


Figure 10. Flow rate of hydrogen in metal hydride during absorption in simulation time 600-s.

3.2. Dynamics of desorption process

3.2.1. Temperature time distribution during desorption

Figure 11 shows, the changes in the temperature at different times during the hydrogen desorption from MHHST. Due to the endothermic nature of the reaction, the desorption of hydrogen at initial stage, which is 0_s is very slow, and the temperature value was noticed to be 293_K, which is the initial temperature of the simulation. As the time increases, the temperature along the MHHST also tends to increase. This is happening up to the 600s. At that time the temperature increases rapidly to much higher values. After a long time the system comes down to thermal equilibrium with the heating fluid. It can be concluded that desorption occurs very fast at higher temperatures with an increase of operating time.

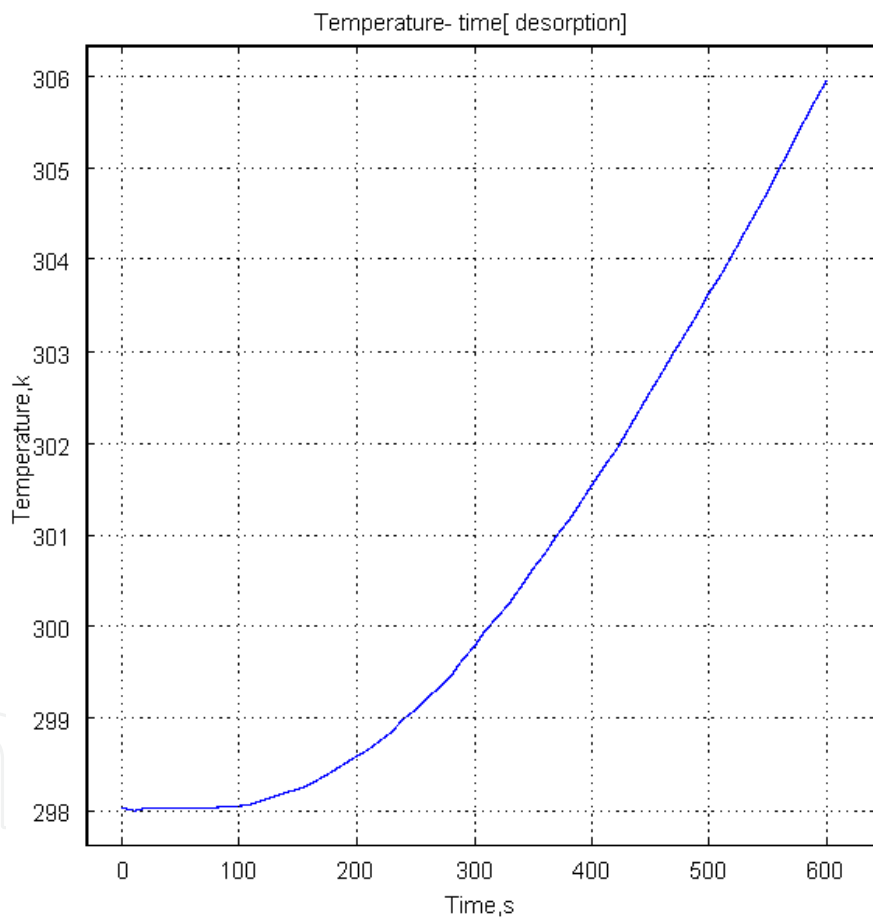


Figure 11. Time evolution of temperature in metal hydride reactor at point with coordinates [0.08, 0.14] during 600s period.

3.2.2. Pressure time distribution during desorption

Figure 12 shows that pressure distributions at the point [0.08, 0.14] within the MHHST during desorption with initial gas phase pressure are set to be 10_bar, which is equal to equilibrium

temperature at 293_K (initial bed temperature). Although the MHHST is operated at 8_bar at the start, the simulation shows that before the average pressure approaches the equilibrium value, only the small amount of hydrogen in gas phase is released and there is no desorption in this period. From Figure 12, we can see that there is initial pressure drop from 8bar to the equilibrium pressure. The focus was based on what happened when desorption start ($t=0$). The discharging pressure is set to be 1_bar. desorption rate increases as the coolant temperature increases, since hydrogen desorption in metal hydride is an endothermic reaction. Moreover the centre temperature drops down right after the desorption reaction occurs.

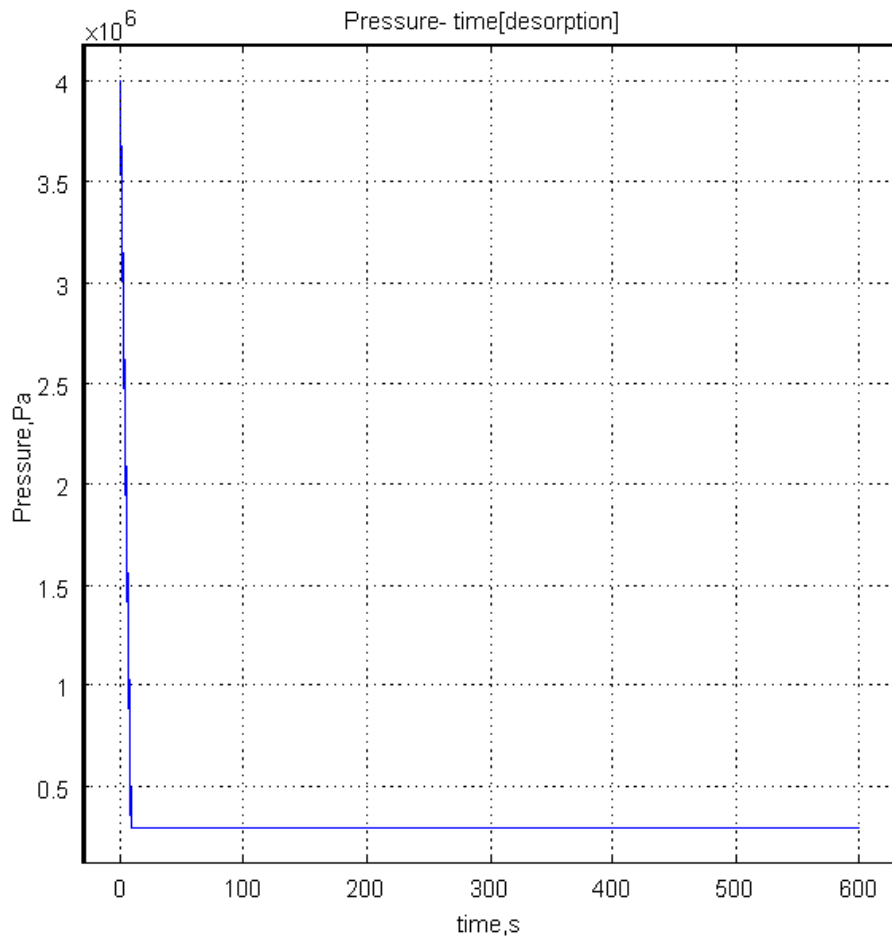


Figure 12. Pressure distribution of hydrogen from metal hydride at [0.08, 0.14] in simulation time 600s during desorption.

3.2.3. Velocity time distribution during desorption

In Figure 13, the velocity of hydrogen released during desorption within MHHST is shown at time interval of 600_s. At a point [0.08, 0.14] inside the MHHST, the velocity of hydrogen increases with increasing simulation time due to endothermic nature of the reaction and tends to decrease further as simulation time is increases. If the desorption temperature varies within the bed and pressure is very low, the velocity of hydrogen increases.

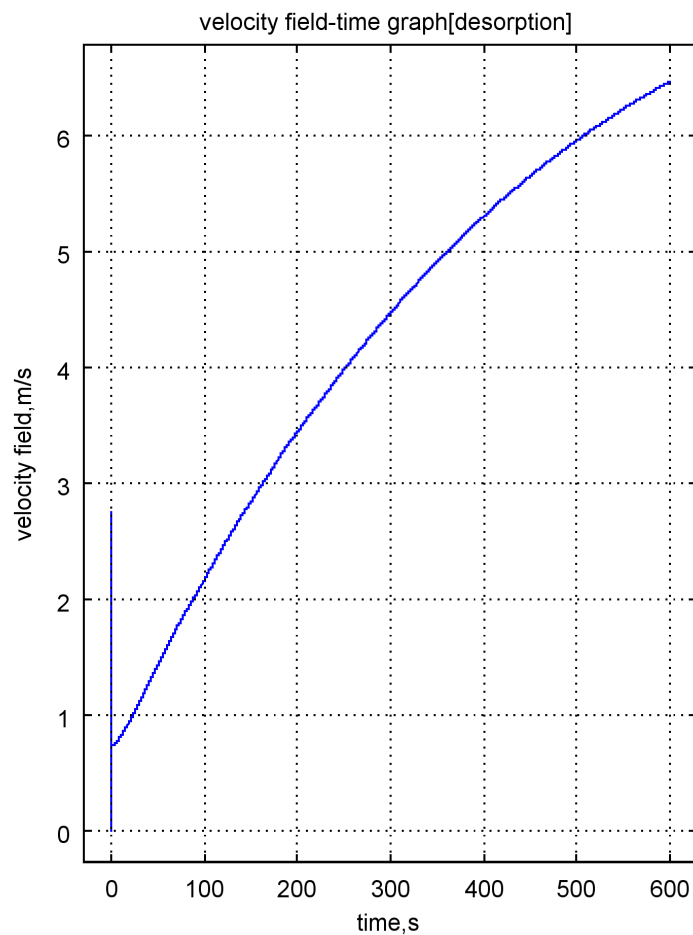


Figure 13. Velocity distribution of hydrogen in metal hydride during desorption.

3.2.4. Concentration distribution

The concentration of hydrogen in metal hydride tank during reaction decreases rapidly with time, as shown in Figure 14. There was a larger percentage of hydrogen in metal hydride storage due to the cold nature of the wall and low heat transfer from the bed to the surrounding cooling fluid, and this was due to low poor thermal conductivity of the metal hydride particles. The concentration of hydrogen decreases as the time increases, and heat distribution within the MHHST also increases. At higher temperature and higher heat transfer coefficient, the concentration of hydrogen in metal hydride decreases with increasing simulation time.

3.2.5. Hydrogen flow rate

The rate of hydrogen desorption from metal hydride storage tank is shown in Figure 15. At the start of the reaction, hydrogen desorption rate is very slow at 0_s, but it increases gradually with time as the tank is heated up at a temperature of 333K. more hydrogen was released from metal hydride hydrogen storage tank. At simulation time of 600_s, larger percentage of hydrogen was released from MHHST, and it is evidence that at increasing simulation time and higher temperature, and low pressure, more hydrogen will be released.

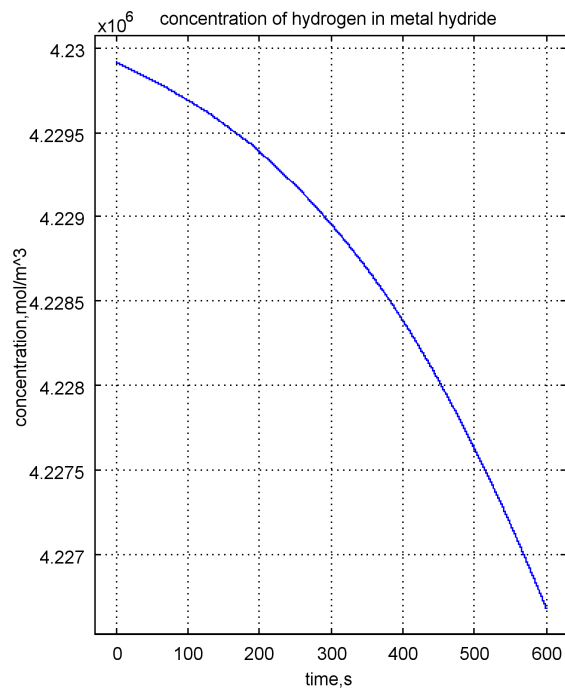


Figure 14. Concentration of hydrogen in metal hydride during desorption at simulation time (600_s).

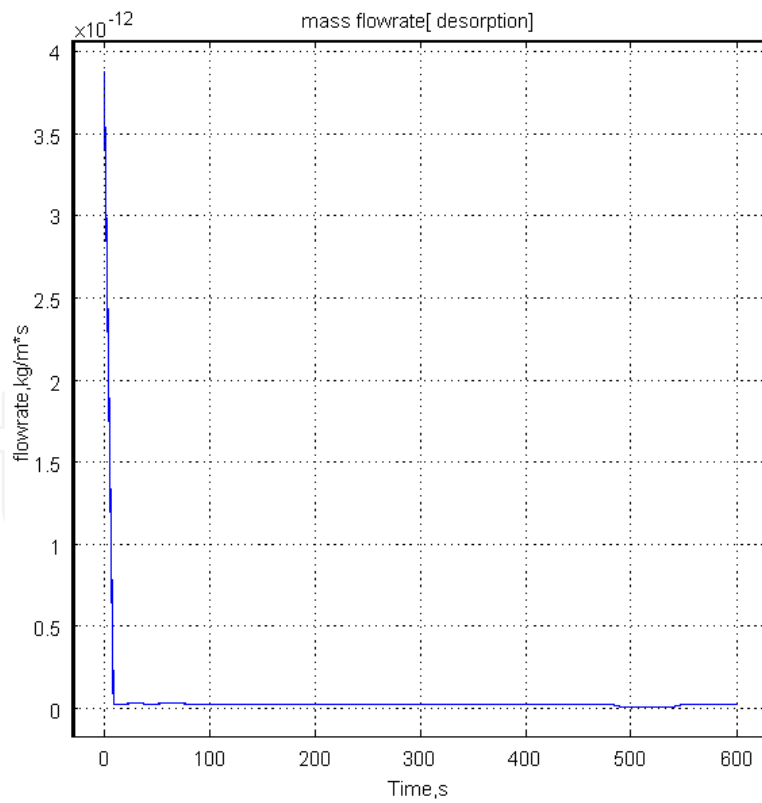


Figure 15. Hydrogen flow rate from metal hydride in simulation time 600s during desorption

3.2.6. Temperature distribution in the tank with fins

Figure 16 shows the temperature distribution within the MHHST during simulation of hydrogen absorption and desorption at simulation time of 600_s. The temperature profile shows two different temperature scales supplied to the system. The temperature supplied by the copper plate to the system, which changes with time along the MHHST, the temperature released by metal hydride when it absorbs/ desorbs hydrogen; it was observed that temperature increases rapidly at different distances of the MHHST. The time taken for the temperature to be released was 551.4_s.

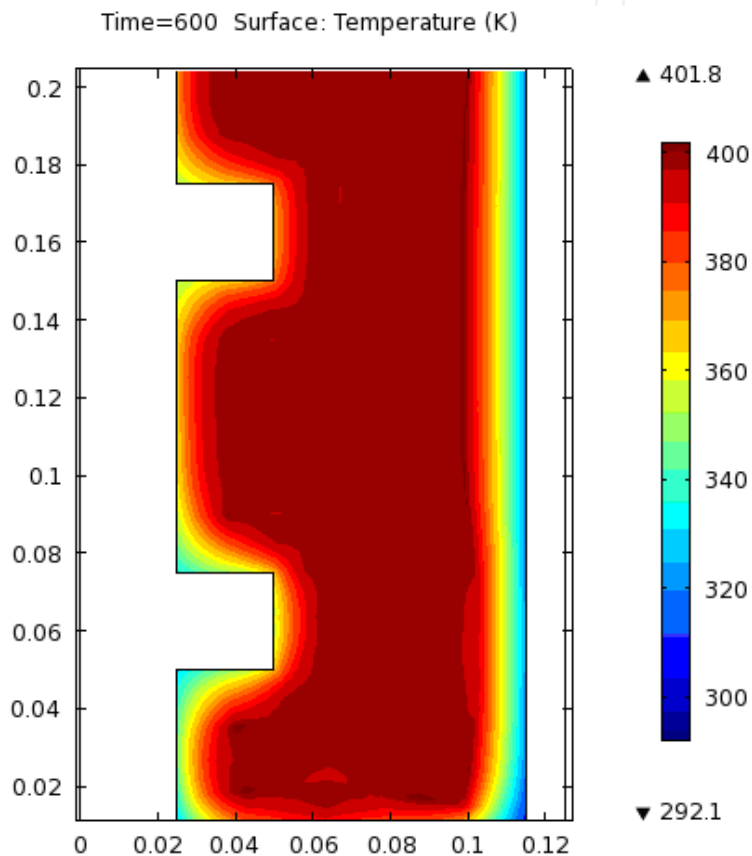


Figure 16. Temperature pattern along the metal hydride hydrogen storage tank.

3.2.7. Pressure profile

Figure 17 shows the pressure distribution in MHHST during the simulation, there is an increase in pressure along different distances within the computational domain of the tank. It was observed that pressure increased rapidly from the equilibrium pressure to the set point pressure of 40 bar at a temperature of 273_K within a simulation time of 600_s for absorption process. In addition, for desorption process, the pressure decreases rapidly from the equilibrium pressure to set point pressure of 10bar at a temperature of 333_K within a simulation time of 600s in the tank due to the endothermic nature of the reaction.

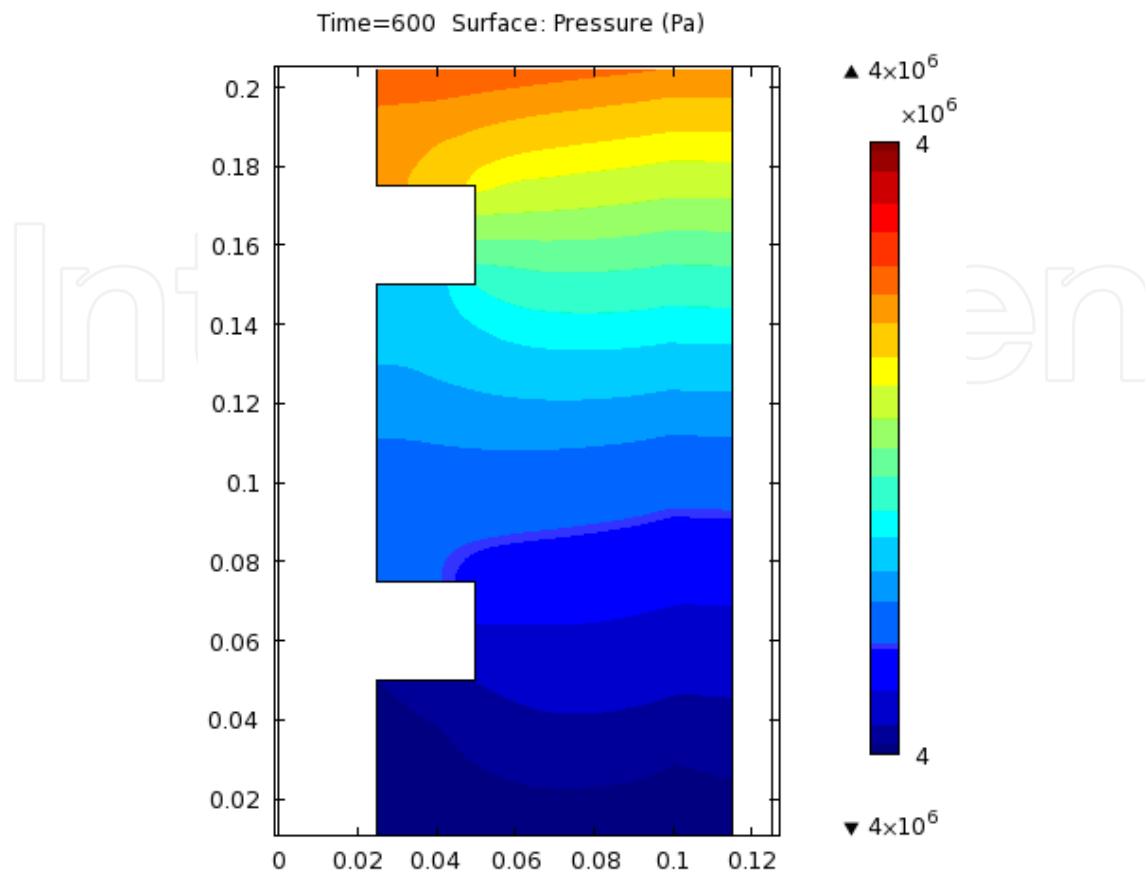


Figure 17. Pressure variation along metal hydride hydrogen storage tank.

4. Conclusions

The objectives of this research have been achieved, thus dynamic mathematical model for the MHHST was developed. The following conclusions can be drawn;

1. In order to verify the model, the numerical model presented above was compared to experimental results of Jemni et al, [3]. The influence of all the operating parameters in the model such as temperature, pressure, density, velocity, and flow rate was investigated. It was found that the pressure and temperature axial distribution in the MHHST for absorption, are in good agreement with the measured experimental values of Jemni et al. [3].
2. The simulations of heat and mass transfer for MHHST with different internal geometries were done. Heat transfer, mass transfer and momentum transfer modules were effectively incorporated in COMSOL Multiphysics 4.0a software. Geometry was built for the problem, and boundary conditions were properly allocated to the each domain in the model. The energy (convection and conduction), mass (diffusion), and momentum (Darcy's law) transport equations and some specific user – defined subroutines were

implemented in the software. It was discovered that the geometry with fins results in faster absorption and desorption when compared with the geometry without fins, in which the absorption/desorption rate is very slow and produce very negligible values for absorption/desorption rate.

3. Temperature, pressure and density non-steady distributions inside the metal hydride porous bed were revealed. It was found that absorption occurs faster at a lower temperature and higher pressure because absorption process is exothermic reaction, and desorption occurs at higher temperature and lower pressure due to the endothermic nature of desorption process. Concentration increases with absorption of hydrogen and decreases with desorption of hydrogen.

5. Abbreviations

2D; Two-Dimensional

PDE; Partial differential Equations

MHHST; Metal hydride hydrogen storage tank

USDE; United States Department of Energy

CFD; Computational Fluid Dynamic

DOE; Department of Energy

PEMFC; Proton exchange membrane fuel cell

ODEs; Ordinary differential equations

HHV; Higher heating value

LHV; Lower heating value

SPEFC; Solid polymer electrolyte fuel cell

MFPM Multi; facilitated proton membrane

DFAFC; Direct formic acid fuel cell

Acknowledgements

The authors will like to express their sincere gratitude to the faculty of Engineering and built environment, Tshwane University of Technology Pretoria South Africa for her financial assistance.

Author details

Olaitan Akanji* and Andrei Kolesnikov

*Address all correspondence to: laitan436us@yahoo.com

Department of Chemical, Metallurgical & Materials Engineering, Tshwane University of Technology, Pretoria, South Africa

References

- [1] Visaria, M., Mudawar, I., Poupont, T., Kumar, S. *Int. J. Heat Mass Trans.* 2010, 53, 2229-2239.
- [2] Zhixiong, G., Hyung, J. S. *J. Int. J. Heat and Mass Trans.* 1999, 42, 379-382.
- [3] JEMNI, A., BEN NASRALLAH, S. Study of two dimensional heat and mass transfer- During adsorption in a metal- hydrogen reactor, *Int. J. Hydrogen Energy* 1995, 20, 43-52. Doi:10.1016/0360-3199(93) E0007-8.
- [4] Aldas, K., MAT M.D. AND KAPLAN, Y. A three dimensional mathematical model for absorption in a metal hydride bed, *Int. J. of Hydrogen Energy* 2002, 27 1049-1056. Doi/10.1016/j.ijhydene.2011.12.140
- [5] Mayer, U., Grill, M. AND Supper, W. Heat and mass transfer in metal hydrides reactions beds, experiment and theoretical results, *J. Less-common Metals* 1987, 131, 238.
- [6] Nakagawa, T., Inomata, A., Aoki, H. & Miura, T. Numerical analysis of heat and mass transfer characteristics in the metal hydride bed. *Int. j. Hydrogen Energy* 2002, 25, 4, 339-350. Doi:-org/10.1016/so360-3199 (99) 0036-1
- [7] Dhaoua, H., Mlloulia, S., Askaria, F., Jemni, A. Ben Nasrallahi, S. *Int. J. Hydrogen Energy* 2007, 32, 1922. Doi:/10.1016/j.ijhydene.2006.08.045.
- [8] Jemni, A., Nasrallah, SB, Lamloumi, J. Experimental and theoretical study of a metal hydrogen reactor, *int. j. of Hydrogen Energy*, 24, 631- 644.
- [9] Chung, C.A., HO, C. J Thermal fluid behavior of the hydriding and dehydrating processes in a metal hydride hydrogen storage. Doi-10.1016/SO360-3199 (01) 0030-1.
- [10] MAT, M.D. AND KAPLAN, Y. Numerical study of hydrogen in a La-Ni₅ hydride Reactor, *Int. J. Hydrogen Energy* 2001, 26, 957.